Role of the Endothelium on Arterial Vasomotion

Michèle Koenigsberger,* Roger Sauser,* Jean-Louis Bény,† and Jean-Jacques Meister*
*Ecole Polytechnique Fédérale de Lausanne, Laboratory of Cell Biophysics, Lausanne, Switzerland; and †Department of Zoology and Animal Biology, University of Geneva, Geneva, Switzerland

ABSTRACT It is well-known that cyclic variations of the vascular diameter, a phenomenon called vasomotion, are induced by synchronous calcium oscillations of smooth muscle cells (SMCs). However, the role of the endothelium on vasomotion is unclear. Some experimental studies claim that the endothelium is necessary for synchronization and vasomotion, whereas others report rhythmic contractions in the absence of an intact endothelium. Moreover, endothelium-derived factors have been shown to abolish vasomotion by desynchronizing the calcium signals in SMCs. By modeling the calcium dynamics of a population of SMCs coupled to a population of endothelial cells, we analyze the effects of an SMC vasoconstrictor stimulation on endothelial cells and the feedback of endothelium-derived factors. Our results show that the endothelium essentially decreases the SMCs calcium level and may move the SMCs from a steady state to an oscillatory domain, and vice versa. In the oscillatory domain, a population of coupled SMCs exhibits synchronous calcium oscillations. Outside the oscillatory domain, the coupled SMCs present only irregular calcium flashings arising from noise modeling stochastic opening of channels. Our findings provide explanations for the published contradictory experimental observations.

INTRODUCTION

Vasomotion is a natural property of many muscular vessels. It consists of cyclic variations of the vascular diameter caused by local changes in contraction and relaxation of smooth muscle cells (SMCs) present in the muscular vessel wall. Arterial contraction has been shown to be due to an increase in the smooth muscle cytosolic calcium concentration (Meininger et al., 1991). Calcium increases result from the presence of vasoconstrictors in the vascular system. In vitro, calcium increases in vascular cells can be induced by receptor-ligand agonists. The latter bind to cell-surface receptors, which activate phospholipase C (PLC) and induce the release of the second messenger, inositol 1,4,5-trisphosphate (IP_3). IP_3 then releases calcium from the intracellular stores (Minneman, 1988). SMCs have to present synchronous calcium oscillations to generate vasomotion, otherwise their calcium dynamics induce only a constant contraction (Mauban et al., 2001; Peng et al., 2001; Sell et al., 2002; Lamboley et al., 2003). The synchronization is achieved via gap junctions, which may mediate electrical, calcium, and IP_3 couplings; for a review see Bény (1999) or Dora (2001).

Endothelial cells (ECs), situated at the interface between the blood and the muscular media, have been shown to play an important role in modulating vascular tone. Myoendothelial gap junctions between SMCs and ECs have been found (Sandow and Hill, 2000), and heterocellular bidirectional communication between SMCs and ECs has been reported (Dora et al., 1997, 2000; Budel et al., 2001; Dora et al., 2003b). Calcium increases in SMCs induce elevated calcium concentrations in ECs. In contrast with SMCs that present synchronous calcium oscillations during vasomotion, experimental observations on rat mesenteric arterial strips (Lamboley et al., 2005) indicate that the ECs calcium concentrations present irregular calcium transients in response to an SMC stimulation during vasomotion. Moreover, experimental evidence suggests that calcium increases in ECs occurring after a calcium increase in SMCs (Lamboley et al., 2005) or astrocytes (Braet et al., 2001) are due to a gap-junctional IP_3 diffusion. High calcium levels in ECs then cause an endothelial hyperpolarization by triggering the efflux of potassium through calcium-activated potassium channels (Baron et al., 1996; Sollini et al., 2002). The calcium increases in ECs lead to the generation of two factors that act on SMCs: endothelium-derived relaxing factor (EDRF), and endothelium-derived hyperpolarizing factor (EDHF). EDRF has been identified as nitric oxide (NO). This gas diffuses rapidly to SMCs and increases cyclic guanosine monophosphate (cGMP) concentration in SMCs. The mediator cGMP decreases the SMC cytosolic calcium level, which causes vasodilation (Ignarro et al., 1986). It acts by enhancing the refilling of intracellular stores (Cohen et al., 1999), activating calcium-sensitive potassium channels (Archer et al., 1994), stimulating Na^+/Ca^{2+} exchange (Furukawa et al., 1991), and inhibiting the generation of IP_3 (Hirata et al., 1990). In contrast to EDRF, the identity of EDHF remains controversial. Recently, there has been evidence that EDHF represents the hyperpolarization spreading electrotonically through myoendothelial gap junctions from ECs to SMCs (Doughty et al., 2000; Coleman et al., 2001; Sandow et al., 2002; Ungvari et al., 2002; Dora et al., 2003a; Griffith et al., 2004). The hyperpolarization then decreases the influx of calcium in SMCs through voltage-operated

Submitted October 22, 2004, and accepted for publication March 22, 2005.
Address reprint requests to Michèle Koenigsberger, Ecole Polytechnique Fédérale de Lausanne (EPFL), Laboratory of Cell Biophysics, CH-1015 Lausanne, Switzerland. Tel.: 41-21-693-8347; Fax: 41-21-693-8305; E-mail: michele.koenigsberger@epfl.ch.

0006-3495/05/06/3845/10 $2.00
doi: 10.1529/biophysj.104.054965

calcium channels (VOCCs), which brings about a vessel relaxation.

The role of the endothelium-derived factors in the generation and maintenance of vasomotion remains unclear (Shimamura et al., 1999). Some experimental studies claim that the presence of endothelium is necessary for vasomotion (Gustafsson et al., 1993; Huang and Cheung, 1997; Peng et al., 2001; Okazaki et al., 2003). However, vasomotion is also observed in the absence of an intact endothelium (Sell et al., 2002; Haddock et al., 2002; Lamboley et al., 2003). Sell et al. (2002) even show that the endothelium can abolish vasomotion by desynchronizing calcium signals in SMCs. To the best of our knowledge, there is no explanation for these contradictory experimental observations.

In this study, we address this point by modeling a population of coupled SMCs and ECs. As an extension of a previous work (Koenigsberger et al., 2004) modeling a population of coupled SMCs, we consider a two-dimensional layer of SMCs superposed on a two-dimensional layer of ECs. First neighboring SMCs and ECs are connected through homocellular and heterocellular gap junctions via electrical, calcium, and IP_3 coupling. We start by considering a single SMC-EC pair to understand how the presence of an EC affects the calcium dynamics of an SMC. The effects of an SMC vasoconstrictor stimulation on the EC and the feedback of the EC (generation of NO and endothelium-induced hyperpolarization) on the SMC is analyzed. The generalization of these results to a population of SMCs and ECs allows us to explain why the endothelium may induce vasomotion in certain circumstances and abolish it in others.

MATHEMATICAL MODEL

Single SMC and EC

In contrast with an SMC, an EC is a non-excitable cell. A calcium rise in an EC is not associated with a membrane potential depolarization (absence of VOCCs) but with a hyperpolarization due to the efflux of potassium through calcium-activated potassium channels (Baron et al., 1996; Sollini et al., 2002). Moreover, a nonspecific cation channel is of significant importance in the EC calcium response (Sollini et al., 2002). Other important cellular mechanisms governing the calcium dynamics in both the SMC and the EC are the calcium release from IP_3- or ryanodine-sensitive stores, the calcium uptake in the sarcoplasmic reticulum/endoplasmic reticulum (SR/ER), the calcium extrusion out of the cytosol (which is voltage-dependent for SMCs; Furukawa et al., 1989), and the leak of calcium from the SR/ER (for a review on calcium entry channels in ECs, see Nilius and Droogmans, 2001).

We use the model of Koenigsberger et al. (2004) to describe the calcium dynamics of a single SMC i. The model has five variables: the calcium concentration in the cytosol c_i; the calcium concentration in the SR s_i; the cell membrane potential v_i; the open state probability w_i of calcium-activated potassium channels; and the IP_3 concentration I_i. This model extends the one of Parthimos et al. (1999, 2003), in which the equations for calcium concentration (c_i and s_i) are based on the two-pool model of Goldbeter et al. (1990).

To describe the calcium dynamics of a single EC j, we construct a similar model based on the equations of Goldbeter et al. (1990). The evolution of EC membrane potential is described by an equation taken from Schuster et al. (2003) that details the calcium-activated potassium channels and reproduces the experimentally observed calcium induced hyperpolarization. The expression of the nonselective cation channel is also taken from Schuster et al. (2003) and added to the equation describing the cytosolic calcium concentration. IP_3 dynamics is described in the same manner as in our SMC model. Thus the EC model has four variables: the cytosolic calcium concentration $\tilde{c}_j$; the calcium concentration in the ER $\tilde{s}_j$; the cell membrane potential $\tilde{v}_j$; and the IP_3 concentration $\tilde{I}_j$.

The SMC model is given by

$$\frac{dc_i}{dt} = J_{IP3_i} - J_{SRuptake_i} + J_{CICR_i} - J_{extrusion_i} + J_{leak_i} - J_{VOCC_i} + J_{Na/Ca_i}, \quad (1)$$

$$\frac{ds_i}{dt} = J_{SRuptake_i} - J_{CICR_i} - J_{leak_i}, \quad (2)$$

$$\frac{dv_i}{dt} = \gamma(-J_{Na/K_i} - J_{Cl_i} - 2J_{VOCC_i} - J_{Na/Ca_i} - J_{K_i}), \quad (3)$$

$$\frac{dw_i}{dt} = \lambda(K_{activation_i} - w_i), \quad (4)$$

$$\frac{dI_i}{dt} = J_{PLC_{agonist_i}} - J_{degrad_i}. \quad (5)$$

The EC model reads

$$\frac{d\tilde{c}_j}{dt} = \tilde{J}_{IP3_j} - \tilde{J}_{ERuptake_j} + \tilde{J}_{CICR_j} - \tilde{J}_{extrusion_j} + \tilde{J}_{leak_j} + \tilde{J}_{cation_j} + \tilde{J}_{0_j}, \quad (6)$$

$$\frac{d\tilde{s}_j}{dt} = \tilde{J}_{ERuptake_j} - \tilde{J}_{CICR_j} - \tilde{J}_{leak_j}, \quad (7)$$

$$\frac{d\tilde{v}_j}{dt} = -\frac{1}{\tilde{C}_m}(\tilde{I}_{K_j} + \tilde{I}_{R_j}), \quad (8)$$

$$\frac{d\tilde{I}_j}{dt} = \tilde{J}_{PLC_{agonist_j}} - \tilde{J}_{degrad_j}. \quad (9)$$

The various terms appearing in these two sets of nonlinear differential equations are detailed in Parthimos et al. (1999) and Koenigsberger et al. (2004) for the SMC model, and Goldbeter et al. (1990) and Schuster et al. (2003) for the EC model. The calcium fluxes

$$J_{IP3_i} = F\frac{I_i^2}{K_r^2 + I_i^2} \text{ and } \tilde{J}_{IP3_j} = \tilde{F}\frac{\tilde{I}_j^2}{\tilde{K}_r^2 + \tilde{I}_j^2} \quad (10)$$

model the calcium release from IP_3-sensitive stores,

$$J_{SRuptake_i} = B\frac{c_i^2}{c_i^2 + c_b^2} \text{ and } \tilde{J}_{ERuptake_j} = \tilde{B}\frac{\tilde{c}_j^2}{\tilde{c}_j^2 + \tilde{c}_b^2} \quad (11)$$

model the SR/ER uptake,

$$J_{CICR_i} = C\frac{s_i^2}{s_c^2 + s_i^2}\frac{c_i^4}{c_c^4 + c_i^4} \text{ and } \tilde{J}_{CICR_j} = \tilde{C}\frac{\tilde{s}_j^2}{\tilde{s}_c^2 + \tilde{s}_j^2}\frac{\tilde{c}_j^4}{\tilde{c}_c^4 + \tilde{c}_j^4} \quad (12)$$

describe the calcium-induced calcium release (CICR),

$$J_{extrusion_i} = Dc_i\left(1 + \frac{v_i - v_d}{R_d}\right) \text{ and } \tilde{J}_{extrusion_j} = \tilde{D}\tilde{c}_j \quad (13)$$

are the calcium extrusion by Ca^{2+}-ATPase pumps,

$$J_{leak_i} = Ls_i \text{ and } \tilde{J}_{leak_j} = \tilde{L}\tilde{s}_j \quad (14)$$

correspond to the leak from the SR/ER,

$$J_{\mathrm{VOCC_i}} = G_{\mathrm{Ca}} \frac{v_\mathrm{i} - v_{\mathrm{Ca_1}}}{1 + e^{-[(v_\mathrm{i} - v_{\mathrm{Ca_2}})/R_{\mathrm{Ca}}]}} \tag{15}$$

is the calcium influx through VOCCs, and

$$J_{\mathrm{Na/Ca_i}} = G_{\mathrm{Na/Ca}} \frac{c_\mathrm{i}}{c_\mathrm{i} + c_{\mathrm{Na/Ca}}} (v_\mathrm{i} - v_{\mathrm{Na/Ca}}) \tag{16}$$

is the Na^+/Ca^{2+} exchange. The term

$$J_{\mathrm{Na/K_i}} = F_{\mathrm{Na/K}} \tag{17}$$

is the Na^+-K^+-ATPase,

$$J_{\mathrm{Cl_i}} = G_{\mathrm{Cl}}(v_\mathrm{i} - v_{\mathrm{Cl}}) \tag{18}$$

models the chloride channels,

$$J_{\mathrm{K_i}} = G_{\mathrm{K}} w_\mathrm{i} (v_\mathrm{i} - v_{\mathrm{K}}) \tag{19}$$

is the K^+ efflux,

$$K_{\mathrm{activation_i}} = \frac{(c_\mathrm{i} + c_\mathrm{w})^2}{(c_\mathrm{i} + c_\mathrm{w})^2 + \beta e^{-[(v_\mathrm{i} - v_{\mathrm{Ca_3}})/R_{\mathrm{K}}]}} \tag{20}$$

describes the calcium and voltage activation of K^+ channels,

$$\tilde{J}_{\mathrm{cation_j}} = \tilde{G}_{\mathrm{cat}}(\tilde{E}_{\mathrm{Ca}} - \tilde{v}_\mathrm{j}) \frac{1}{2} \left(1 + \tanh\left(\frac{\log_{10} \tilde{c}_\mathrm{j} - \tilde{m}_{3_{\mathrm{cat}}}}{\tilde{m}_{4_{\mathrm{cat}}}} \right) \right) \tag{21}$$

is the calcium influx through two non-selective cation channels, $\tilde{J}_{0_\mathrm{j}}$ regroups further calcium influx (assumed constant) to the cell,

$$\tilde{\mathcal{I}}_{\mathrm{K_j}} = \tilde{G}_{\mathrm{tot}}(\tilde{v}_\mathrm{j} - \tilde{v}_{\mathrm{K}})(\tilde{\mathcal{I}}_{\mathrm{BK_{Ca_j}}} + \tilde{\mathcal{I}}_{\mathrm{SK_{Ca_j}}}) \tag{22}$$

is the potassium efflux through the BK_{Ca} channel (a large conductance channel activated by calcium and membrane potential) and the SK_{Ca} channel (a small-conductance channel only activated by calcium), with

$$\tilde{\mathcal{I}}_{\mathrm{BK_{Ca_j}}} = \frac{0.4}{2} \left(1 + \tanh\left(\frac{(\log_{10} \tilde{c}_\mathrm{j} - \tilde{c})(\tilde{v}_\mathrm{j} - \tilde{b}) - \tilde{a}_1}{\tilde{m}_{3\mathrm{b}}(\tilde{v}_\mathrm{j} + \tilde{a}_2(\log_{10} \tilde{c}_\mathrm{j} - \tilde{c}) - \tilde{b})^2 + \tilde{m}_{4\mathrm{b}}} \right) \right) \tag{23}$$

and

$$\tilde{\mathcal{I}}_{\mathrm{SK_{Ca_j}}} = \frac{0.6}{2} \left(1 + \tanh\left(\frac{\log_{10} \tilde{c}_\mathrm{j} - \tilde{m}_{3\mathrm{s}}}{\tilde{m}_{4\mathrm{s}}} \right) \right). \tag{24}$$

The residual current regrouping Cl^- and Na^+ currents is written

$$\tilde{\mathcal{I}}_{\mathrm{R_j}} = \tilde{G}_{\mathrm{R}}(\tilde{v}_\mathrm{j} - \tilde{v}_{\mathrm{rest}}), \tag{25}$$

and the IP_3 fluxes

$$J_{\mathrm{degrad_i}} = kI_\mathrm{i} \text{ and } \tilde{J}_{\mathrm{degrad_j}} = \tilde{k}\tilde{I}_\mathrm{j} \tag{26}$$

model the IP_3 degradation. The constants $J_{\mathrm{PLC_{agonist_i}}}$ and $\tilde{J}_{\mathrm{PLC_{agonist_j}}}$ are the rate of PLC activated by agonists. Thus a raise in SMC vasoconstrictor concentration is simulated by an increase of the PLC rate $J_{\mathrm{PLC_{agonist_i}}}$. In the following we do not consider EC stimulation by agonists and $\tilde{J}_{\mathrm{PLC_{agonist_j}}}$ is set to zero.

The parameter values of the SMC model are taken from Koenigsberger et al. (2004) and are given in Table 1. The EC parameter values appearing in the equation for membrane potential (Eq. 8) and in term $\tilde{J}_{\mathrm{cation_j}}$ (term 21) are taken from Schuster et al. (2003). These values fit experimental results describing calcium-induced hyperpolarization. On the other hand, to the best of our knowledge, the amplitudes $\tilde{F}$, $\tilde{B}$, $\tilde{C}$, $\tilde{D}$, and $\tilde{L}$ are not known. These amplitudes and all the other parameter values of the terms present in both SMC and EC models are chosen the same as for the SMC model, except for the amplitudes $\tilde{B}$ and $\tilde{C}$ of the terms $\tilde{J}_{\mathrm{ERuptake_j}}$ (term 11) and $\tilde{J}_{\mathrm{CICR_j}}$ (term 12). These terms are responsible for calcium oscillations, and we choose to decrease them so that ECs present only transient calcium increases at all levels of IP_3 or calcium concentrations. A summary of the

TABLE 1 Parameter values for the single SMC model

Parameter	Description	Value
F	Maximal rate of activation-dependent calcium influx	0.23 μM/s
K_r	Half saturation constant for agonist-dependent calcium entry	1 μM
G_{Ca}	Whole cell conductance for VOCCs	0.00129 μM mV^{-1} s^{-1}
$v_{\mathrm{Ca_1}}$	Reversal potential for VOCCs	100.0 mV
$v_{\mathrm{Ca_2}}$	Half-point of the VOCC activation sigmoidal	−24.0 mV
R_{Ca}	Maximum slope of the VOCC activation sigmoidal	8.5 mV
$G_{\mathrm{Na/Ca}}$	Whole cell conductance for Na^+/Ca^{2+} exchange	0.00316 μM mV^{-1} s^{-1}
$c_{\mathrm{Na/Ca}}$	Half-point for activation of Na^+/Ca^{2+} exchange by Ca^{2+}	0.5 μM
$v_{\mathrm{Na/Ca}}$	Reversal potential for the Na^+/Ca^{2+} exchanger	−30.0 mV
B	SR uptake rate constant	2.025 μM/s
c_b	Half-point of the SR ATPase activation sigmoidal	1.0 μM
C	CICR rate constant	55 μM/s
s_c	Half-point of the CICR Ca^{2+} efflux sigmoidal	2.0 μM
c_c	Half-point of the CICR activation sigmoidal	0.9 μM
D	Rate constant for Ca^{2+} extrusion by the ATPase pump	0.24 s^{-1}
v_d	Intercept of voltage dependence of extrusion ATPase	−100.0 mV
R_d	Slope of voltage dependence of extrusion ATPase	250.0 mV
L	Leak from SR rate constant	0.025 s^{-1}
γ	Scaling factor relating net movement of ion fluxes to the membrane potential (inversely related to cell capacitance)	1970 mV/μM
$F_{\mathrm{Na/K}}$	Net whole cell flux via the Na^+-K^+-ATPase	0.0432 μM/s
G_{Cl}	Whole cell conductance for Cl^- current	0.00134 μM mV^{-1} s^{-1}
v_{Cl}	Reversal potential for Cl^- channels	−25.0 mV
G_{K}	Whole cell conductance for K^+ efflux	0.00446 μM mV^{-1} s^{-1}
v_{K}	Reversal potential for K^+	−94.0 mV
λ	Rate constant for net K_{Ca} channel opening	45.0
c_w	Translation factor for Ca^{2+} dependence of K_{Ca} channel activation sigmoidal	0 μM
β	Translation factor for membrane potential dependence of K_{Ca} channel activation sigmoidal	0.13 μM^2
$v_{\mathrm{Ca_3}}$	Half-point for the K_{Ca} channel activation sigmoidal	−27.0 mV
R_{K}	Maximum slope of the K_{Ca} activation sigmoidal	12.0 mV
k	Rate constant of IP_3 degradation	0.1 s^{-1}

EC parameter values is given in Table 2. As membrane channels open and close stochastically at finite temperature, a Gaussian noise is added into the parameter values. The noise level is chosen to obtain variances for model curves comparable to experimental data (Koenigsberger et al., 2004).

Intercellular communication

For intercellular communication, we consider homocellular (SMC-SMC, EC-EC) and heterocellular (SMC-EC) electrical, calcium, and IP_3 coupling. To simplify our study, gap junctions between two neighboring cells are modeled by a single global conductance or permeability, which is supposed to be the same in every direction, even if the contact surface between adjacent cells is variable. All heterocellular coupling coefficients are assumed to be symmetric. Apart from these gap-junctional couplings, we also consider the effects of the endothelium-derived NO on SMCs.

Homocellular communication

Between SMCs

A term

$$V_{\text{coupling}_i} = -g\sum_k (v_i - v_k) \tag{27}$$

TABLE 2 Parameter values for the single EC model

Parameter	Description	Value
$\tilde{F}$	Maximal rate of activation-dependent calcium influx	0.23 μM/s
$\tilde{K}_r$	Half saturation constant for agonist-dependent calcium entry	1 μM
$\tilde{B}$	ER uptake rate constant	0.5 μM/s
$\tilde{c}_b$	Half-point of the ER ATPase activation sigmoidal	1.0 μM
$\tilde{C}$	CICR rate constant	5 μM/s
$\tilde{s}_c$	Half-point of the CICR Ca^{2+} efflux sigmoidal	2.0 μM
$\tilde{c}_c$	Half-point of the CICR activation sigmoidal	0.9 μM
$\tilde{D}$	Rate constant for Ca^{2+} extrusion by the ATPase pump	0.24 s^{-1}
$\tilde{L}$	Leak from ER rate constant	0.025 s^{-1}
$\tilde{k}$	Rate constant of IP_3 degradation	0.1 s^{-1}
$\tilde{G}_{cat}$	Whole-cell cation channel conductivity	0.66 nM mV^{-1} s^{-1}
$\tilde{E}_{Ca}$	Ca^{2+} equilibrium potential	50 mV
$\tilde{m}_{3_{cat}}$		-0.18 μM
$\tilde{m}_{4_{cat}}$		0.37 μM
$\tilde{J}_{0_j}$	Constant calcium influx	0.029 μM/s
$\tilde{C}_m$	Membrane capacitance	25.8 pF
$\tilde{G}_{tot}$	Total potassium channel conductivity	6927 pS
$\tilde{v}_K$	K^+ equilibrium potential	-80 mV
$\tilde{a}_1$		53.3 μM mV
$\tilde{a}_2$		53.3 mV/μM
$\tilde{b}$		-80.8 mV
$\tilde{c}$		-0.4 μM
$\tilde{m}_{3b}$		1.32×10^{-3} μM/mV
$\tilde{m}_{4b}$		0.30 μM mV
$\tilde{m}_{3s}$		-0.28 μM
$\tilde{m}_{4s}$		0.389 μM
$\tilde{G}_R$	Residual current conductivity	955 pS
$\tilde{v}_{rest}$	Membrane resting potential	-31.1 mV

is added for each SMC i to Eq. 3 to model the electrical coupling with all nearest-neighboring SMCs k. The gap-junctional electrical coupling coefficient g is related to the gap-junctional conductance G by $g = G/C_m$, where C_m is the cell membrane capacitance. The calcium coupling describing calcium diffusion is modeled by a term

$$J_{\text{c-coupling}_i} = -p\sum_k (c_i - c_k), \tag{28}$$

complementing Eq. 1. The IP_3 coupling describing IP_3 diffusion is modeled by a term

$$J_{\text{I-coupling}_i} = -p_{IP_3}\sum_k (I_i - I_k) \tag{29}$$

added to Eq. 5. The coupling coefficients are set to $g = 1000\ s^{-1}$, $p = 0.05\ s^{-1}$, and $p_{IP3} = 0\ s^{-1}$ (Koenigsberger et al., 2004).

Between ECs

A term

$$\tilde{V}_{\text{coupling}_j} = -\tilde{g}\sum_l (\tilde{v}_j - \tilde{v}_l) \tag{30}$$

is added for each EC j to Eq. 8 to model the electrical coupling with all nearest-neighboring ECs l. Setting $\tilde{C}_m \simeq 3 \times 10^{-5}$ μF (Schuster et al., 2003) and $\tilde{G} \simeq 30$ nS (Van Rijen et al., 1997) gives a gap-junctional electrical coupling coefficient $\tilde{g}$ of the order of 1000 s^{-1}. The terms modeling calcium and IP_3 coupling are set to zero, since they are not known. We will come back to this choice in Results and Discussion.

Heterocellular communication

To model heterocellular electrical coupling, the terms

$$V^{\text{SMC-EC}}_{\text{coupling}_i} = -\hat{g}\sum_l (v_i - \tilde{v}_l) \text{ and } V^{\text{EC-SMC}}_{\text{coupling}_j} = -\hat{g}\sum_k (\tilde{v}_j - v_k) \tag{31}$$

are added to Eqs. 3 and 8, respectively. The values represented by $\tilde{v}_l$ are membrane potentials of the neighboring ECs l of SMC i, whereas the values represented by v_k are membrane potentials of the neighboring SMCs k of EC j. Setting $C_m \simeq \tilde{C}_m \simeq 2 \times 10^{-5}$ μF (Parthimos et al., 1999; Schuster et al., 2003) and $\hat{G} \simeq 1$ nS (Yamamoto et al., 2001) gives a gap-junctional electrical coupling coefficient $\hat{g}$ of the order of 50 s^{-1}. The calcium coupling describing calcium diffusion is modeled by the terms

$$J^{\text{SMC-EC}}_{\text{c-coupling}_i} = -\hat{p}\sum_l (c_i - \tilde{c}_l) \text{ and } J^{\text{EC-SMC}}_{\text{c-coupling}_j} = -\hat{p}\sum_k (\tilde{c}_j - c_k) \tag{32}$$

added to Eqs. 1 and 6, respectively. The IP_3 coupling describing IP_3 diffusion is modeled by the terms

$$J^{\text{SMC-EC}}_{\text{I-coupling}_i} = -\hat{p}_{IP_3}\sum_l (I_i - \tilde{I}_l) \text{ and } J^{\text{EC-SMC}}_{\text{I-coupling}_j} = -\hat{p}_{IP_3}\sum_k (\tilde{I}_j - I_k) \tag{33}$$

added to Eqs. 5 and 9, respectively. We choose to set the heterocellular coupling coefficients $\hat{p}$ to zero and $\hat{p}_{IP_3}$ to 0.05 s^{-1}. Other possibilities will be addressed in Results and Discussion.

NO acts on SMCs by enhancing the refilling of intracellular stores, activating calcium-sensitive potassium channels, stimulating Na^+/Ca^{2+} exchange, and inhibiting the generation of IP_3. Its effects can thus be simulated by increasing the value of parameters B, G_K, and $G_{Na/Ca}$ in terms 11, 19, and 16, and by decreasing $J_{\text{PLC}_{\text{agonist}_i}}$.

Numerical methods

The model equations were solved using a fourth-order Runge-Kutta method. For populations of cells, the equations were integrated on a two-dimensional grid of rectangular SMCs superposed on a two-dimensional grid of rectangular ECs (Fig. 1). Within each SMC and EC, the calcium and membrane potential dynamics are described by Eqs. 1–5 and Eqs. 6–9, respectively. Each cell is connected with its nearest neighbors on the same layer (homocellular communication, terms 27–30) and with the cells on the other layer directly superposed on it (heterocellular communication, terms 31–33). The software AUTO, as implemented in XPPAUT by B. Ermentrout (http://www.pitt.edu/~phase/), was used for bifurcation diagrams. All stable solutions indicated by AUTO have been found in our numerical simulations.

RESULTS AND DISCUSSION

Single cell

SMC

The behavior of the cytosolic calcium concentration c_i of an isolated SMC i with respect to the agonist activated PLC-rate, $J_{PLC_{agonist_i}}$, is shown on Fig. 2. At low values of $J_{PLC_{agonist_i}}$ (i.e., at low vasoconstrictor concentration), the cytosolic calcium level is in a stable steady state (domain I on Fig. 2). Increasing the vasoconstrictor concentration, one reaches a Hopf bifurcation: the steady state becomes unstable and the calcium level begins to oscillate (domain II on Fig. 2). Our simulations show that the mean calcium level and the frequency of the oscillations become higher with increasing values of $J_{PLC_{agonist_i}}$. Finally, there is a second Hopf bifurcation from which the steady state becomes stable again (domain III on Fig. 2). Note that a calcium rise in the SMC is accompanied by a membrane potential depolarization, due to the presence of VOCCs (term 15) (see also Fig. 3 of Koenigsberger et al., 2004). The introduction of a Gaussian noise in parameter values results in a few irregular calcium flashes in the SMC at low vasoconstrictor concentrations in the domain I on Fig. 2 (see also Fig. 2 *b* of Koenigsberger et al., 2004): the calcium level may exceed a threshold and flash at moments distributed stochastically in time. Introduction of noise at higher values of $J_{PLC_{agonist_i}}$ results in small fluctuations between two calcium oscillations (domain II; see also Fig. 2 *c* of Koenigsberger et al. (2004)) or around the steady state (domain III; see also Fig. 2 *d* of Koenigsberger et al. (2004)).

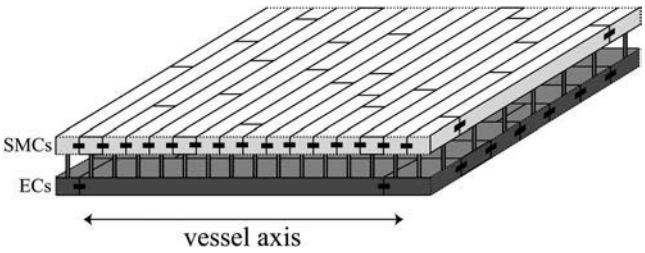

FIGURE 1 The model equations are integrated on a two-dimensional grid of SMCs superposed on a two-dimensional grid of ECs (the third dimension is for visualization purposes only). ECs are arranged parallel, and SMCs perpendicular, to the vessel axis. Cell geometry is approximated by a rectangle. The width of an EC is taken to be twice that of an SMC, and the length of an EC is taken to be 1.3 times that of an SMC (Sandow and Hill, 2000). The cell geometry only plays a role in determining the number of neighbors: each SMC generally has six nearest-neighboring SMCs and 5–6 nearest-neighboring ECs, and each EC generally has six nearest-neighboring ECs and ~15 nearest-neighboring SMCs. Each cell is connected with its nearest neighbors on the same layer (homocellular connection, –) and with the cells on the other layer directly superposed on it (heterocellular connection, ||).

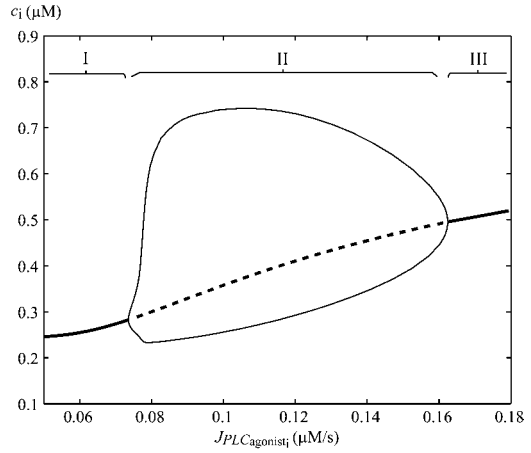

FIGURE 2 Bifurcation diagram for the cytosolic calcium concentration c_i of an isolated SMC with respect to the rate of PLC $J_{PLC_{agonist_i}}$ (*thick solid line*, stable rest state; *thick dashed line*, unstable rest state; and *thin solid line*, minima and maxima of stable oscillations). Two Hopf bifurcations divide the diagram into three domains (domains I and III, steady state; and domain II, oscillations).

EC

With the parameter values chosen, the EC model exhibits no calcium oscillations. The calcium level is in a stable steady state at all values of IP_3 concentration $\tilde{I}_j$. Introducing a Gaussian noise in parameter values results in few irregular calcium fluctuations and flashings of the EC. An elevated calcium level is associated with a membrane potential hyperpolarization, whose major compound can be inhibited by blocking the SK_{Ca} channel (i.e., by setting term 24 to zero).

Single SMC-EC pair

An elevated calcium level in an SMC induces irregular calcium flashings (resulting from noise) in a neighboring EC via heterocellular chemical coupling. Electrical coupling leads to membrane potential values that are similar for the SMC and the EC. The calcium increases in the EC lead to a membrane potential hyperpolarization due to potassium efflux through the SK_{Ca} channel (term 24). Moreover, a high calcium level in the EC leads to the generation of NO that can be simulated in our model by increasing B, G_K, or $G_{Na/Ca}$, and by decreasing $J_{PLC_{agonist_i}}$.

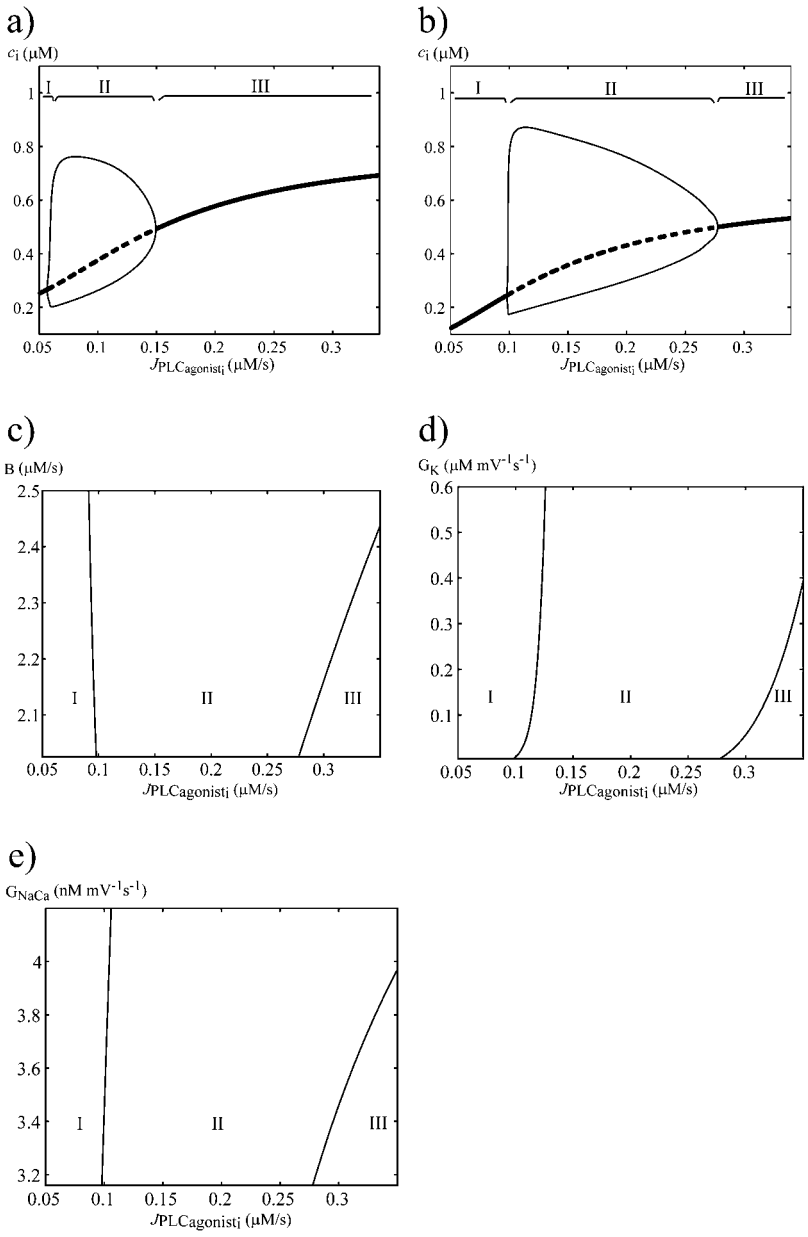

FIGURE 3 Bifurcation diagrams of an SMC coupled to an EC. (*a–b*) Bifurcation diagrams for the SMC cytosolic calcium concentration c_i with respect to the rate of PLC $J_{PLC_{agonist_i}}$ (*thick solid line*, stable rest state; *thick dashed line*, unstable rest state; and *thin solid line*, minima and maxima of stable oscillations). On panel *a*, the major part of the EC hyperpolarization is inhibited (i.e., the SK_{Ca} channel is blocked) and the effects of NO are not taken into account (i.e., parameters B, G_K, and $G_{Na/Ca}$ are unchanged). On panel *b*, the SK_{Ca} channel is open in the absence of NO. (*c–e*) Two-parameter bifurcation diagrams showing the evolution of the two Hopf bifurcations with the rate of NO (simulated by an increase of B, G_K, and $G_{Na/Ca}$, respectively) and the rate of PLC $J_{PLC_{agonist_i}}$. On these diagrams the SK_{Ca} channel is open.

The bifurcation diagram of Fig. 3 *a* shows the SMC calcium concentration with respect to the agonist-activated PLC rate. For this simulation, the SK_{Ca} channel is blocked and the parameters B, G_K, and $G_{Na/Ca}$ are not modified. This figure then simulates a situation in which the major effects of the endothelium (EC hyperpolarization and NO) are not taken into account. There is an oscillatory domain (domain II) and two steady-state domains (domains I and III). Note that because of the electrical and IP_3 coupling with the EC, the bifurcation diagram of Fig. 3 *a* is slightly different from the one of an isolated SMC (Fig. 2). On the diagram of Fig. 3 *b*, we focus on the effects of the hyperpolarization: the SK_{Ca} channel is open in the absence of NO. The hyperpolarization propagates to the SMC (term 31). It then lowers the mean calcium level of the SMC by decreasing the calcium influx through VOCCs (term 15). With respect to Fig. 3 *a* the mean calcium level is decreased, the three domains (I, II, and III) are shifted to the right, and domain II has become larger. In the two-parameter bifurcation diagrams of Fig. 3, *c–e*, the SK_{Ca} channel is open and the action of NO is analyzed by increasing parameters B, G_K, or $G_{Na/Ca}$ with respect to Table 1. An increase in B increases the range of $J_{PLC_{agonist_i}}$ corresponding to domain II (Fig. 3 *c*), but the SMC calcium level remains unchanged. Increasing G_K or $G_{Na/Ca}$ decreases the mean calcium level by shifting the domains I, II, and III to the right and enlarges domain II (Fig. 3, *d* and *e*). At a fixed value of $J_{PLC_{agonist_i}}$ in domain II, increasing B, G_K, and $G_{Na/Ca}$ increases the amplitude of the oscillations and decreases their

frequency. Another effect of NO is to inhibit IP_3 generation. In our model, this can be simulated by decreasing $J_{PLC_{agonist_i}}$, and simply leads to a decrease of the mean SMC calcium level.

Population of SMCs and ECs, and comparison with experiments

In a population of coupled SMCs and ECs under uniform SMC vasoconstrictor stimulation, we still observe the three domains described in Fig. 2. As for a population of SMCs without ECs (Koenigsberger et al., 2004), the calcium oscillations in domain II are synchronous, whereas the irregular flashings in domain I are essentially asynchronous with the SMC coupling coefficients values used. The results obtained in the case of an SMC-EC pair can be generalized to a population of SMCs and ECs. The major effect of the endothelium on a population of SMCs is to decrease the SMC calcium level. This has been observed experimentally; see, for instance, Fig. 4 of Gustafsson et al. (1993), Fig. 1 *b* of Gustafsson et al. (1994), Fig. 6 of Budel et al. (2001), or Fig. 2 *a* of Okazaki et al. (2003). Domain II is smaller if the effects of the endothelium are not taken into account, which may explain why some experimental studies do not observe synchronous calcium oscillations giving rise to vasomotion in the absence of endothelium at the vasoconstrictor concentrations they have chosen. Within domain II the endothelium decreases the frequency of the SMC calcium oscillations and increases their amplitude, but their synchronization is preserved. This is in agreement with experimental observations. For instance, Kasai et al. (1997) have observed that under electrical or noradrenaline stimulation the frequency of the calcium oscillations of SMCs decreased when ECs were stimulated with acetylcholine, which increases the EC cytosolic calcium concentration (see Fig. 2 *E* of Kasai et al., 1997). The frequency was also lowered in the presence of NO donor sodium nitroprusside (see Fig. 4, *C* and *D*, of Kasai et al., 1997). The endothelium-induced calcium decrease in SMCs shifts the domains I, II, and III to the right. A direct consequence of this domain shifting is that the endothelium can induce oscillatory behavior in a non-oscillating SMC population (transition from domain III to domain II), or suppress oscillations by initiating a transition from domain II to domain I.

The endothelium may induce vasomotion

An example of a transition from domain III to domain II is given on Fig. 4, *a* and *b*. A uniform stimulation by an SMC vasoconstrictor at $J_{PLC_{agonist_i}} = 0.29\,\mu M/s$ leads to a high non-oscillating calcium level in the SMCs if the major effects of the endothelium are not taken into account, i.e., the SK_{Ca} channel is blocked and the effects of NO are not taken into account. Experimentally, a high calcium level in SMCs

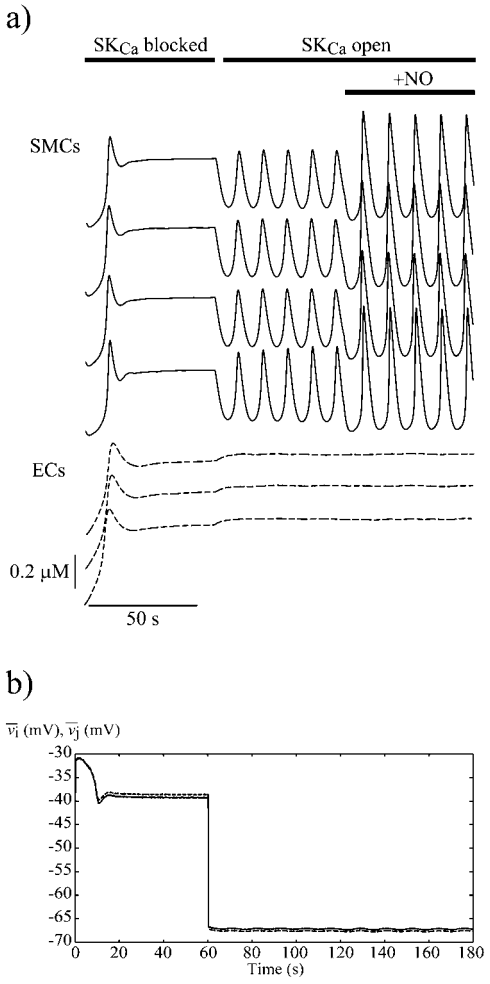

FIGURE 4 Time courses for a coupled population of ~60 SMCs and ~30 ECs (with $J_{PLC_{agonist_i}} = 0.29\,\mu M/s$). The uniform SMC vasoconstrictor stimulation begins at $t = 0$ s. During the period indicated by the first bar, the major part of the EC hyperpolarization is inhibited (i.e., the SK_{Ca} channel is blocked) and the effects of NO are not taken into account (i.e., parameters B, G_K, and $G_{Na/Ca}$ are unchanged). In a second step, the SK_{Ca} channel is open in the absence of NO. Finally, the SK_{Ca} channel is held open and the parameter B is increased to simulate the action of NO on the SMCs ($B = 2.5\,\mu M/s$). (*a*) Evolution of the cytosolic calcium concentrations of four representative SMCs (*solid curves*) and three ECs (*dashed curves*). (*b*) Evolution of the mean SMC membrane potential $\overline{v_i}$ (*solid curve*) and the mean EC membrane potential $\overline{v_j}$ (*dashed curve*). The mean is taken over the entire grid.

corresponds to a tonic contraction (Lamboley et al., 2003). Electrical coupling results in membrane potential values for SMCs and ECs that are similar, as observed experimentally (Emerson and Segal, 2000). The SK_{Ca} channel is then open in the absence of NO. The EC hyperpolarization propagating to the SMCs decreases the calcium level sufficiently to bring about oscillations in SMCs. With the SMC coupling coefficients used, these oscillations are synchronous. Experimentally synchronous SMC calcium oscillations give rise to vasomotion (Lamboley et al., 2003). Note that the EC calcium level has become higher: the EC hyperpolarization

increases the EC calcium level due to an increased calcium influx through the nonselective cation channel (term 21). Finally, the SK_{Ca} channel is held open and the action of NO is simulated by an elevated value of B ($B = 2.5\ \mu$M/s). The SMC calcium oscillations are still synchronous. Their amplitude increases and their frequency decreases.

Experimentally, the reverse transition (from domain II to domain III) has been observed by Dora et al. (2000) by inhibiting the effects of the endothelium. In Fig. 1 of Dora et al. (2000), endothelium intact vessels stimulated by a certain dose of phenylephrine (PE) presented vasomotion. PE acts only on SMCs and not on ECs (Dora et al., 2000) by binding to α-adrenoceptors. After adding N^{ω}-nitro-L-arginine methyl ester, a blocker of NO-synthesis, the average contraction was increased. The amplitude and frequency of the oscillations was decreased and increased, respectively. The addition of charybdotoxin (a nonselective inhibitor of BK_{Ca} channels acting on SMCs and ECs) abolished vasomotion and further increased the contraction. Apamin (an inhibitor of the SK_{Ca} channel) further augmented the contraction to PE. These behaviors correspond to the ones simulated on Fig. 4 in the reverse order (the effect of inhibiting all large conductance potassium channels is not shown on the figure).

In Fig. 1 *E* of the study of Peng et al. (2001), vasomotion was also observed in the presence of endothelium under norepinephrine stimulation. After endothelium removal, the calcium level was more elevated and SMCs presented asynchronous calcium increases. In our interpretation, such flashings result from the stochastic opening of channels. The removal of endothelium corresponds to a transition from domain II to domain III in our model. To analyze the effect of NO, Peng et al. (2001) then added an analog of cGMP, 8-bromo-cGMP, and they observed that vasomotion reappears, which can be interpreted as a transition from domain III to domain II.

In Fig. 1 of the study of Gustafsson et al. (1993), removing the endothelium also increases the contraction and abolishes vasomotion, which corresponds to the transition from domain II to domain III.

The endothelium may abolish vasomotion

An example of a transition from domain II to domain I is given on Fig. 5, *a* and *b*. A uniform stimulation by an SMC vasoconstrictor at $J_{PLC_{agonist_i}} = 0.127\,\mu$M/s leads to an oscillating calcium level in the SMCs if the SK_{Ca} channel is blocked in the absence of NO. With the SMC coupling coefficients used, these oscillations are synchronous and experimentally this gives rise to vasomotion. SMCs membrane potential oscillations are transmitted to the ECs. The SK_{Ca} channel is then open in the absence of NO. The SMC calcium oscillations are still synchronous. The hyperpolarization propagating to the SMCs decreases the frequency of the SMC calcium oscillations, and increases their amplitude.

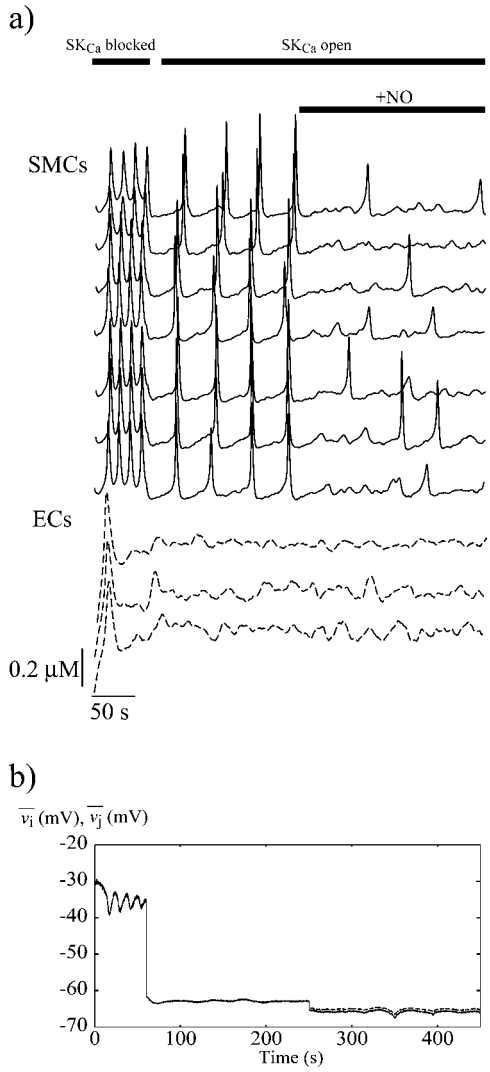

FIGURE 5 Time courses for a coupled population of ~60 SMCs and ~30 ECs (with $J_{PLC_{agonist_i}} = 0.127\ \mu$M/s). The uniform SMC vasoconstrictor stimulation begins at $t = 0$ s. During the period indicated by the first bar, the major part of the EC hyperpolarization is inhibited (i.e., the SK_{Ca} channel is blocked) and the effects of NO are not taken into account (i.e., parameters B, G_K, and $G_{Na/Ca}$ are unchanged). In a second step, the SK_{Ca} channel is open in the absence of NO. Finally, the SK_{Ca} channel is held open, and the parameter G_K is increased to simulate the action of NO on the SMC ($G_K = 0.2\ \mu$M mV^{-1} s^{-1}). (*a*) Evolution of the cytosolic calcium concentrations of seven representative SMCs (*solid curves*) and three ECs (*dashed curves*). (*b*) Evolution of the mean SMC membrane potential $\overline{v_i}$ (*solid curve*) and the mean EC membrane potential $\overline{v_j}$ (*dashed curve*). The mean is taken over the entire grid.

The SMC membrane potential oscillations are attenuated because of the EC hyperpolarization propagating to the SMCs. Finally, the SK_{Ca} channel is held open and the action of NO is simulated by an increase of parameter G_K ($G_K = 0.2\ \mu$M mV^{-1} s^{-1}). This decreases the SMC calcium level further and induces a transition from domain II to domain I of Fig. 3 *d*. The SMCs no longer oscillate, but present only few flashings due to noise modeling stochastic opening of

channels. These flashings are essentially asynchronous with the coupling coefficients used. Thus the endothelium can have a ''desynchronizing effect'' on the calcium signals of SMCs. Note that the EC calcium level is lower and more sensitive to noise on Fig. 5 than on Fig. 4 because the SMC vasoconstrictor concentration (i.e., term $J_{\mathrm{PLC}_{\mathrm{agonist_i}}}$) is lower.

Experimentally, this ''desynchronizing effect'', corresponding to a transition from domain II to domain I, has been observed by Sell et al. (2002), who obtained vasomotion both in the presence and the absence of endothelium. The synchronization of the calcium signals was attenuated by acetylcholine acting on ECs (see Fig. 6 of Sell et al., 2002) and SMCs then presented only irregular flashings. Sell et al. (2002) observed that the synchronization was augmented by adding the NO inhibitor N^{ω}-nitro-L-arginine methyl ester. This manipulation corresponds to a transition from domain I to II.

Nature of EDHF

We have shown that the hyperpolarization propagating from ECs to SMCs through myoendothelial gap junctions can model the experimental behaviors attributed to EDHF. Our model then supports the hypothesis about the nature of EDHF proposed by many authors (Doughty et al., 2000; Coleman et al., 2001; Sandow et al., 2002; Ungvari et al., 2002; Dora et al., 2003a; Griffith et al., 2004).

Consequences of different model hypotheses

We have chosen to base the EC model on the equations of Goldbeter et al. (1990) and Schuster et al. (2003), but our results do not depend qualitatively on the precise calcium dynamics of each single EC. In particular, we have verified that our findings remain qualitatively the same if the EC model is modified to allow calcium oscillations. Moreover, the exact values for calcium or IP_3 coupling between ECs are not known. Experimentally, it has been observed that a local calcium increase in ECs does not propagate at long distances (Dora et al., 2003b), which is the case when calcium and IP_3 couplings are set to zero. Non-zero values for these couplings would only synchronize the ECs calcium concentrations.

Changing the values of the myoendothelial coupling coefficients or the nature of the messenger inducing a calcium rise in ECs following an SMCs calcium increase does not qualitatively affect our results. Decreasing the heterocellular IP_3 coupling coefficient $\hat{p}_{IP_3}$ leads to a lower calcium level in ECs during SMC vasoconstrictor stimulation. The resulting hyperpolarization is then attenuated, which leads to a smaller decrease in the SMC calcium level. Setting $\hat{p}_{IP_3}$ to zero, we observe that a calcium coupling coefficient higher than $0.02\ s^{-1}$ may also induce a calcium rise in ECs following an SMCs calcium increase. A consequence of decreasing the heterocellular electrical coupling coefficient $\hat{g}$ is that the EC hyperpolarization is transmitted to a lesser extent to the SMCs, which, in turn, also decreases the SMC calcium level less. Moreover, the SMC membrane potential oscillations (Fig. 5 *b*) are then attenuated less.

SUMMARY

SMCs may be in a low-calcium-level steady state (domain I), present calcium oscillations (domain II), or be in a high-calcium-level steady state (domain III). In domain II, the SMC coupling coefficients synchronize the calcium oscillations giving rise to vasomotion. In domains I and III, the calcium flashings and fluctuations arising from the stochastic opening of channels cannot be synchronized by these coupling coefficients. We have observed that the endothelium-derived factors (EDHF and NO) increase the range of agonist concentrations for which SMCs present synchronous oscillations: domain II is smaller if the effects of the endothelium are not taken into account (Fig. 3). This may explain why some experimental studies do not observe vasomotion in the absence of endothelium at the vasoconstrictor concentrations they have chosen.

The main effect of the endothelium is to decrease the mean calcium level in SMCs. As a consequence, the endothelium can give rise to vasomotion by inducing a transition from domain III to domain II (Fig. 4). On the other hand, the endothelium may abolish vasomotion by inducing a transition from domain II to domain I (Fig. 5). These two types of transitions provide explanations for the seemingly contradictory experimental observations about the role of the endothelium on vasomotion. The effect of the endothelium is always the same, only the initial conditions, which may depend on the experimental setup (temperature, wall tension, etc.) and the type of vessel, are different: in some experiments, the vessels are prepared so that they are in a steady state, whereas in others they are in an oscillatory state. Our conclusions do not depend on precise details of the model, as long as the SMC presents oscillatory and steady-state behaviors and the EC decreases the SMC calcium level.

This research was supported by Swiss National Science Foundation grant No. FN 31-61716.

REFERENCES

Archer, S. L., J. M. Huang, V. Hampl, D. P. Nelson, P. J. Shultz, and E. K. Weir. 1994. Nitric oxide and cGMP cause vasorelaxation by activation of a charybdotoxin-sensitive K channel by cGMP-dependent protein kinase. *Proc. Natl. Acad. Sci. USA.* 91:7583–7587.

Baron, A., M. Frieden, F. Chabaud, and J. L. Bény. 1996. Ca^{2+}-dependent non-selective cation and potassium channels activated by bradykinin in Pig coronary artery endothelial cells. *J. Physiol.* 493:691–706.

Bény, J. L. 1999. Information networks in the arterial wall. *News Physiol. Sci.* 14:68–73.

Braet, K., K. Paemeleire, K. D'Herde, M. J. Sanderson, and L. Leybaert. 2001. Astrocyte-endothelial cell calcium signals conveyed by two signalling pathways. *Eur. J. Neurosci.* 13:79–91.

Budel, S., A. Schuster, N. Stergiopoulos, J. J. Meister, and J. L. Bény. 2001. Role of smooth muscle cells on endothelial cell cytosolic free calcium in porcine coronary arteries. *Am. J. Physiol.* 281:H1156–H1162.

Cohen, R. A., R. M. Weisbrod, M. Gericke, M. Yaghoubi, C. Bierl, and V. M. Bolotina. 1999. Mechanism of nitric oxide-induced vasodilatation: refilling of intracellular stores by sarcoplasmic reticulum Ca^{2+} ATPase and inhibition of store-operated Ca^{2+} influx. *Circ. Res.* 84:210–219.

Coleman, H. A., M. Tare, and H. C. Parkington. 2001. EDHF is not K^+ but may be due to spread of current from the endothelium in Guinea-pig arterioles. *Am. J. Physiol.* 280:H2478–H2483.

Dora, K. A. 2001. Intercellular Ca^{2+} signalling: the artery wall. *Semin. Cell Dev. Biol.* 12:27–35.

Dora, K. A., M. P. Doyle, and B. R. Duling. 1997. Elevation of intracellular calcium in smooth muscle causes endothelial cell generation of NO in arterioles. *Proc. Natl. Acad. Sci. USA.* 94:6529–6534.

Dora, K. A., J. M. Hinton, S. D. Walker, and C. J. Garland. 2000. An indirect influence of phenylephrine on the release of endothelium-derived vasodilators in Rat small mesenteric artery. *Br. J. Pharmacol.* 129:381–387.

Dora, K. A., S. L. Sandow, N. T. Gallagher, H. Takano, N. M. Rummery, C. E. Hill, and C. J. Garland. 2003a. Myoendothelial gap junctions may provide the pathway for EDHF in Mouse mesenteric artery. *J. Vasc. Res.* 40:480–490.

Dora, K. A., J. Xia, and B. R. Duling. 2003b. Endothelial cell signaling during conducted vasomotor responses. *Am. J. Physiol.* 285:H119–H126.

Doughty, J. M., J. P. Boyle, and P. D. Langton. 2000. Potassium does not mimic EDHF in rat mesenteric arteries. *Br. J. Pharmacol.* 130:1174–1182.

Emerson, G. G., and S. S. Segal. 2000. Electrical coupling between endothelial cells and smooth muscle cells in Hamster feed arteries: role in vasomotor control. *Circ. Res.* 87:474–479.

Furukawa, K., N. Ohshima, Y. Tawada-Iwata, and M. Shigekawa. 1991. Cyclic GMP stimulates Na^+/Ca^{2+} exchange in vascular smooth muscle cells in primary culture. *J. Biol. Chem.* 266:12337–12341.

Furukawa, K., Y. Tawada-Iwata, and M. Shigekawa. 1989. Modulation of plasma membrane Ca^{2+} pump by membrane potential in cultured vascular smooth muscle cells. *J. Biochem. (Tokyo).* 106:1068–1073.

Goldbeter, A., G. Dupont, and M. J. Berridge. 1990. Minimal model for signal-induced Ca^{2+} oscillations and for their frequency encoding through protein phosphorylation. *Proc. Natl. Acad. Sci. USA.* 87:1461–1465.

Griffith, T. M., A. T. Chaytor, and D. H. Edwards. 2004. The obligatory link: role of gap junctional communication in endothelium-dependent smooth muscle hyperpolarization. *Pharmacol. Res.* 49:551–564.

Gustafsson, H., A. Bulow, and H. Nilsson. 1994. Rhythmic contractions of isolated, pressurized small arteries from Rat. *Acta Physiol. Scand.* 152:145–152.

Gustafsson, H., M. J. Mulvany, and H. Nilsson. 1993. Rhythmic contractions of isolated small arteries from Rat: influence of the endothelium. *Acta Physiol. Scand.* 148:153–163.

Haddock, R. E., G. D. Hirst, and C. E. Hill. 2002. Voltage independence of vasomotion in isolated irideal arterioles of the Rat. *J. Physiol.* 540:219–229.

Hirata, M., K. P. Kohse, C. H. Chang, T. Ikebe, and F. Murad. 1990. Mechanism of cyclic GMP inhibition of inositol phosphate formation in Rat aorta segments and cultured bovine aortic smooth muscle cells. *J. Biol. Chem.* 265:1268–1273.

Huang, Y., and K. K. Cheung. 1997. Endothelium-dependent rhythmic contractions induced by cyclopiazonic acid in Rat mesenteric artery. *Eur. J. Pharmacol.* 332:167–172.

Ignarro, L. J., R. G. Harbison, K. S. Wood, and P. J. Kadowitz. 1986. Activation of purified soluble guanylate cyclase by endothelium-derived relaxing factor from intrapulmonary artery and vein: stimulation by acetylcholine, bradykinin and arachidonic acid. *J. Pharmacol. Exp. Ther.* 237:893–900.

Kasai, Y., T. Yamazawa, T. Sakurai, Y. Taketani, and M. Iino. 1997. Endothelium-dependent frequency modulation of Ca^{2+} signalling in individual vascular smooth muscle cells of the Rat. *J. Physiol.* 504:349–357.

Koenigsberger, M., R. Sauser, M. Lamboley, J. L. Bény, and J. J. Meister. 2004. Ca^{2+} dynamics in a population of smooth muscle cells: modeling the recruitment and synchronization. *Biophys. J.* 87:92–104.

Lamboley, M., P. Pittet, M. Koenigsberger, R. Sauser, J. L. Bény, and J. J. Meister. 2005. Evidence for signaling via gap junctions from smooth muscle to endothelial cells in Rat mesenteric arteries: possible implication of a second messenger. *Cell Calcium.* 37:311–320.

Lamboley, M., A. Schuster, J. L. Bény, and J. J. Meister. 2003. Recruitment of smooth muscle cells and arterial vasomotion. *Am. J. Physiol.* 285: H562–H569.

Mauban, J. R., C. Lamont, C. W. Balke, and W. G. Wier. 2001. Adrenergic stimulation of Rat resistance arteries affects Ca^{2+} sparks, Ca^{2+} waves, and Ca^{2+} oscillations. *Am. J. Physiol.* 280:H2399–H2405.

Meininger, G. A., D. C. Zawieja, J. C. Falcone, M. A. Hill, and J. P. Davey. 1991. Calcium measurement in isolated arterioles during myogenic and agonist stimulation. *Am. J. Physiol.* 261:H950–H959.

Minneman, K. P. 1988. Alpha 1-adrenergic receptor subtypes, inositol phosphates, and sources of cell Ca^{2+}. *Pharmacol. Rev.* 40:87–119.

Nilius, B., and G. Droogmans. 2001. Ion channels and their functional role in vascular endothelium. *Physiol. Rev.* 81:1415–1459.

Okazaki, K., S. Seki, N. Kanaya, J. Hattori, N. Tohse, and A. Namiki. 2003. Role of endothelium-derived hyperpolarizing factor in phenylephrine-induced oscillatory vasomotion in Rat small mesenteric artery. *Anesthesiology.* 98:1164–1171.

Parthimos, D., D. H. Edwards, and T. M. Griffith. 1999. Minimal model of arterial chaos generated by coupled intracellular and membrane Ca^{2+} oscillators. *Am. J. Physiol.* 277:H1119–H1144.

Parthimos, D., D. H. Edwards, and T. M. Griffith. 2003. Shil'nikov homoclinic chaos is intimately related to type-III intermittency in isolated rabbit arteries: role of nitric oxide. *Phys. Rev. E Stat. Nonlin. Soft Matter Phys.* 67:051922.

Peng, H., V. Matchkov, A. Ivarsen, C. Aalkjaer, and H. Nilsson. 2001. Hypothesis for the initiation of vasomotion. *Circ. Res.* 88:810–815.

Sandow, S. L., and C. E. Hill. 2000. Incidence of myoendothelial gap junctions in the proximal and distal mesenteric arteries of the Rat is suggestive of a role in endothelium-derived hyperpolarizing factor-mediated responses. *Circ. Res.* 86:341–346.

Sandow, S. L., M. Tare, H. A. Coleman, C. E. Hill, and H. C. Parkington. 2002. Involvement of myoendothelial gap junctions in the actions of endothelium-derived hyperpolarizing factor. *Circ. Res.* 90:1108–1113.

Schuster, A., J. L. Bény, and J. J. Meister. 2003. Modelling the electrophysiological endothelial cell response to bradykinin. *Eur. Biophys. J.* 32:370–380.

Sell, M., W. Boldt, and F. Markwardt. 2002. Desynchronising effect of the endothelium on intracellular Ca^{2+} concentration dynamics in vascular smooth muscle cells of Rat mesenteric arteries. *Cell Calcium.* 32:105–120.

Shimamura, K., F. Sekiguchi, and S. Sunano. 1999. Tension oscillation in arteries and its abnormality in hypertensive animals. *Clin. Exp. Pharmacol. Physiol.* 26:275–284.

Sollini, M., M. Frieden, and J. L. Bény. 2002. Charybdotoxin-sensitive small conductance K_{Ca} channel activated by bradykinin and substance P in endothelial cells. *Br. J. Pharmacol.* 136:1201–1209.

Ungvari, Z., A. Csiszar, and A. Koller. 2002. Increases in endothelial Ca^{2+} activate K_{Ca} channels and elicit EDHF-type arteriolar dilation via gap junctions. *Am. J. Physiol.* 282:H1760–H1767.

Van Rijen, H., M. J. van Kempen, L. J. Analbers, M. B. Rook, A. C. van Ginneken, D. Gros, and H. J. Jongsma. 1997. Gap junctions in human umbilical cord endothelial cells contain multiple connexins. *Am. J. Physiol.* 272:C117–C130.

Yamamoto, Y., M. F. Klemm, F. R. Edwards, and H. Suzuki. 2001. Intercellular electrical communication among smooth muscle and endothelial cells in Guinea-pig mesenteric arterioles. *J. Physiol.* 535:181–195.